

Experimental Investigation on Post-fire Behaviour of Thin-walled Stainless Steel Bolted Connections

Salah Ganem*, Mohammed Mahmood

Department of Civil Engineering, College of Engineering, University of Diyala, 32001
Diyala, Iraq

Abstract:

The use of stainless steel as a structural element became quite common due to its excellent corrosion resistance, durability, and aesthetic appeal. This research performs post-fire testing of austenitic stainless steel bolted connections. The specimens were heated to 800°C and 1000°C for different times (30, 60, 90, and 120 minutes) and cooled by air-cooled or water. Results showed that there is no corrosion in the specimens occurred as a result of water cooling. The ultimate strength decreased by 7% and 12%, when the specimens were heated to 800°C and 1000°C and cooled by air and decreases by 8% and 5% when to cooled with water respectively. The method of cooling did not affect the ultimate strength significantly as the results remained close for both methods of cooling. The AISC approach underestimates the connection post-fire strength.

Keywords: stainless steel, post-fire, bolted connections.

DOI: [10.24297/j.cims.2023.5.28](https://doi.org/10.24297/j.cims.2023.5.28)

1. Introduction

Buildings have utilized stainless steel since the start of the 20th century " Baddoo,2008;Rossi,2014" . It was used for architectural decoration. Then the use of stainless steel as a structural component became widespread. The long life and low maintenance of stainless steel over its lifespan cover its initial high cost, as well as the aesthetic advantages of architecture. "Kim and kuwamure (2007)" investigated the structural behaviour of bolted shear connections in thin-walled stainless steel plates using a finite element. They confirmed that the curling results in 4–25% reduction in ultimate strength. "Kim et al.(2015)" tested single shear bolted connections with four bolts in thin-walled carbon steel to determine fracture mechanism and curling influence on ultimate strength. Using three types of plate thickness (1.5 mm, 3.0 mm and 6.0 mm), and end distance was ranging from 24 mm to 60 mm parallel to load in the test specimen. Curling occurred in thin-walled carbon steel bolted connections with a long end distance and thinner plate. The curling reduces the ultimate strength of the connections. For bolted connections with typical block shear and significant curling, modified

strength formulae were recommended. "Ahmed and Teh (2019)" studied the effects of bolt threads on single and double shear bolted connections. Threaded bolts had lower initial stiffness and higher displacement than half-thread bolts. "Kim et al. (2020)" used parametric finite element analysis to test the structural behaviour of four-bolted connections made of lean duplex stainless steel. The end distance perpendicular to the direction of applied load and edge distance parallel to that direction were the major parameters. It was found that curling decreases ultimate strength by up to 29%. A modified equation was proposed that takes into account both the actual fracture mode at the ultimate state and the impact curling has on strength. "Mahmood et al. (2020)" used finite element to study the effect of end distance on the ultimate strength and fracture sequence of single shear bolt connections of thin-walled carbon steels. The study recommended end distance of 42 mm for plates with a thickness of less than 3.5 mm and 48 mm for thick plates to avoid curling. The maximum distance is 50 mm, as it is not possible to obtain an improvement in strength beyond this limit. The stresses are concentrated between the bolts and the edge of the plate in the direction of the loading. The curling failure leads to a decrease in the strength of the connection by 12%. "Sobrinho et al. (2022)" aimed performing experimental and numerical tests to clarify the response of splice connections. The work involved stainless steel thin plates connected by a single bolt. It was found that curling does not affect the connection strength at the ratio $e/d > 3.5$, and as the thickness of the specimen increases, the effect of curling decreases." "He et al. (2019)" investigated the behaviour of square stainless steel tubular (SSST) stub columns after elevated temperatures under axial compression. It was discovered that high temperature had the largest effect on the columns' ultimate load-bearing capacity. With an increase in the high temperatures the ratio of decrease in carrying capacity, ductility, and initial compressive hardness increased significantly." "Bouchair et al. (2008)" studied the behaviour of stainless steel bolted connections using experimental testing and finite element. The bolts are stressed in shear or tension. The failure types were net section failure and bearing failure. The numerical specimen demonstrated ductile behaviour with improved resistance compared to carbon steel because of strain hardening." "Kim et al. (2011)" studied the strength and curling failure in thin-walled carbon steel bolted connection. All specimens failed in block shear fracture. The ultimate strength decrease ratio varied from 4% to 17% as the end distance increased." "Yang et al. (2013)" calculated the optimal end distance and number of bolts if a steel structure was subjected to fire. The specimen was evaluated by a tensile test at room temperature, after heating to temperatures ranging from 100°C to 650°C. The research advised using a minimum end distance of $3d$ (diameter of bolte) to prevent the plate from ripping. It was also determined

that under fire circumstances, strength grows linearly with an end distance of $4d$." He and Wang (2016)" investigated the behaviour of thin-walled bolted plates at high temperatures. End distances varied from 3diameter bolt to 6diameter bolt, with temperatures rising steadily from 20°C to 700°C . According to the findings, displacement is exactly proportional to temperature increase." Cai and Young (2018)" investigated the single-shear bolted of cold-formed stainless steel (CFSS) connections at high temperatures. Using the ABAQUS software, the finite element model was developed and verified by the existing single shear bolted connection tests. It was suggested that the bearing strengths based on the comparable plastic stresses in the bolt hole may be computed using the proposed bearing factor of 2 with a resistance factor of 0.65. The bearing strengths with considering 6.4mm bolt hole deformation was also suggested." Liu et al. (2017)" carried out an experimental study on slip resistance and shear behaviour of high-strength bolted connections after fire. Diameter of the bolts was 16 mm. The temperature was between (400°C - 900°C). The specimens cooled in air. The reduction factor after 900°C of slip resistance was 0.35, and the reduction factor of shear capacity under the same temperature was 0.75. " Cai and Young (2020)" investigated how temperature and end distance affect thin sheet steel single shear bolted connections. The connection specimens of thickness 0.42 mm G550 and 1.90 mm G450 were employed. The specimens were examined at five temperatures, between 22°C to 900°C . At high temperatures, all specimens failed in a plate bearing with end distances of 3 and 5 d (bolt diameter). According to the research, ultimate loads rise with increasing end distance and eventually reach three times the diameter of the bolt. The high temperature may greatly influence the residual strength and behaviour of the connections. Temperature up to 1000°C at a fire in the buildings" Beitel and Iwankiw (2008)" . There have been few studies on the behaviour of stainless steel bolted connections after elevated temperatures. Therefore the purpose of this study is to provide a fundamental understanding of the post-fire behaviour of stainless steel single shear bolted connections.

2. Experimental study

2.1 Specimens dimension

The experimental programme includes testing of coupons and bolted connections specimens. The dimension of coupons have been used according to EN 10002-1:2001 " EN (2001)" the coupons shown in Figure (1), the specimens shown in Figure (2). Use stainless steel (304), which has a thickness of 4 mm. The specimens were fixed by four bolts 14 mm in diameter. Using a pulling plate with dimensions ($300\text{ mm} \times 180\text{ mm}$) and a thickness of 15 mm to fixing the specimens and ensure its failure in the test shown in Figure(3).

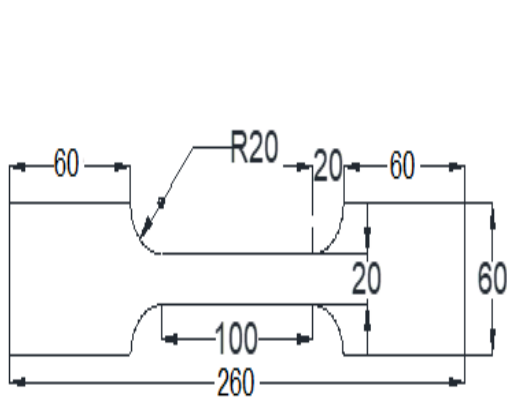


Figure (1) coupon dimensions

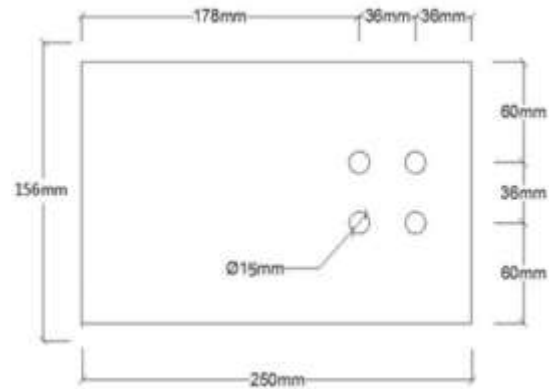


Figure (2) specimen geometry

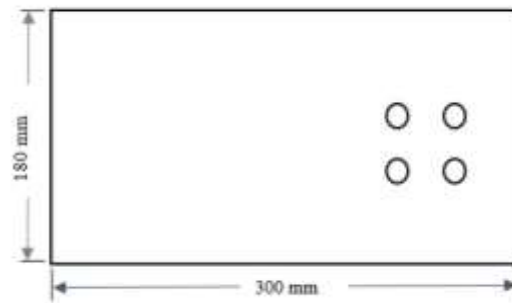


Figure (3) Pulling plate

The coupons and specimens were named based on the specimens tested. The thickness of coupons and specimens is 4mm, as shown in table (1). For example, Cst4 h1000 t30 CW, (C) means coupon, (s) means stainless steel, (t4) means the thickness of specimens, (h1000) 1000°C is the heating temperature of the specimen, (t30) means the heating duration in the furnace is 30 min, (CW) means cooled in water or (CA) means cooled in air.

2.2 Heating and cooling

Coupons and specimens were heated to 800 °C and 1000 °C, and a heating time (30 min, 60 min, 90 min, 120 min), as shown in Figure (4), and then cooled in air or water.



Figure (4) Coupons and specimens heated in a Furnace

3. Results and discussions

3.1 Physical changes

The dimensions of the coupons and specimens were measured by a digital vernier. It was measured in three places to verify the dimensions before and after heating to high temperatures, where it was found that the only decrease was in the thickness. The highest decrease in thickness was approximately 5%, at a temperature of 1000°C at a time of heating 120 min, and the change in thickness of the coupons was the same in the specimens. There was a change in the colour of the specimens as a result of heating and cooling, where the colour of the coupons and specimens changed from the silvery to grey colour and then to dark grey and the appearance of crusts at a heating temperature of 1000°C, as shown in Figure (5).



(a) silver colour

(b) grey colour

(c) grey dark and crusts

Figure (5) The change in the colour of the specimens

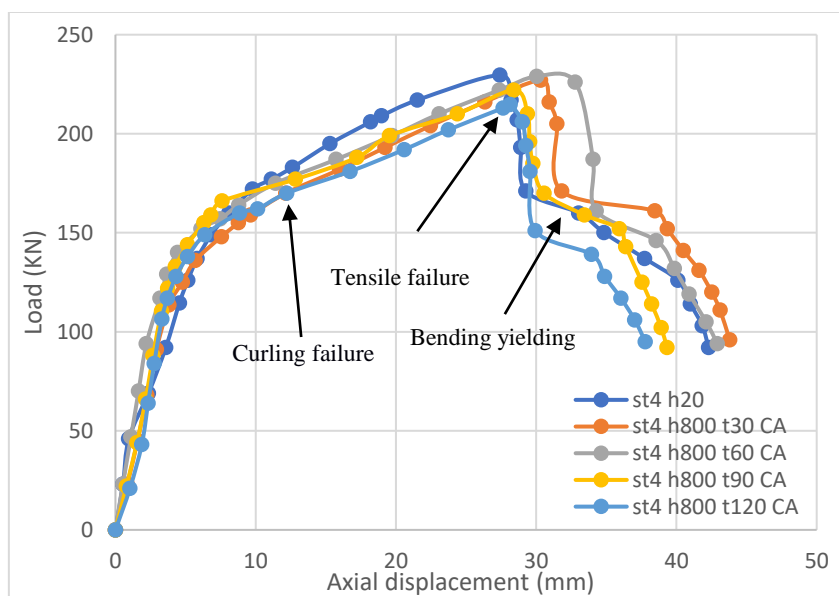
3.2 The Effect of Heating Time at 800°C

Table (1) shows the results of 4mm thickness specimens heated to 800°C and cooled air. As heating duration increases, heated specimen yield load remains close to the reference specimen. The ultimate strength ratio (P_{ut}/P_u) and yield strength ratio (P_{yt}/P_y) dropped by 7% and 6%, respectively, after 120 minutes of heating. Figure (6-a) shows that the axial displacement of specimens heated for 30 and 60 minutes was greater than that of the reference specimen, but it was reduce at 90 min and 120 min. With increased heating times, the ductility increase compared to the reference specimen. As shown in Figure (6-b), the yield strain of the heated specimens is close to the yield strain of the reference specimen. Figure (6-c) shows that the curling displacement of specimens heated at 30 min and 60 min is less than that of the reference specimen, but approaches at 90 min and 120 min. The ratio (P_c/P_u) increases with the increase in the heating period, where the highest ratio decrease is 9% in the heating time 30 min and the lowest decrease is 2% in the heating time 120 min. The curling displacement begins to appear before the specimens have moved into a plastic area, as shown in Figure (6-d).

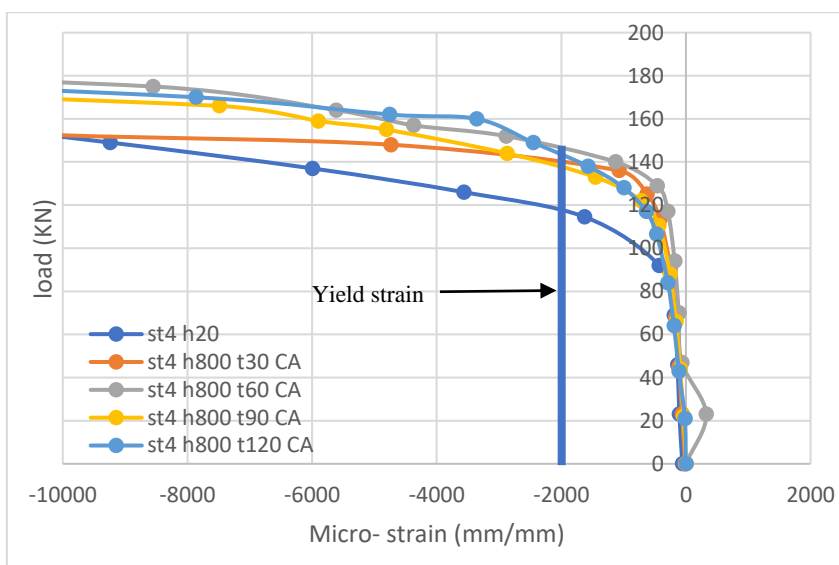
Table (1) The results specimens thickness 4mm-800°C, air-cooled.

Specimen	Yielding Load P_y (kN)	Ultimate Load P_u (kN)	Curling displacement (mm) at max	Curling Load (kN)	P_c/P_u	Ductility

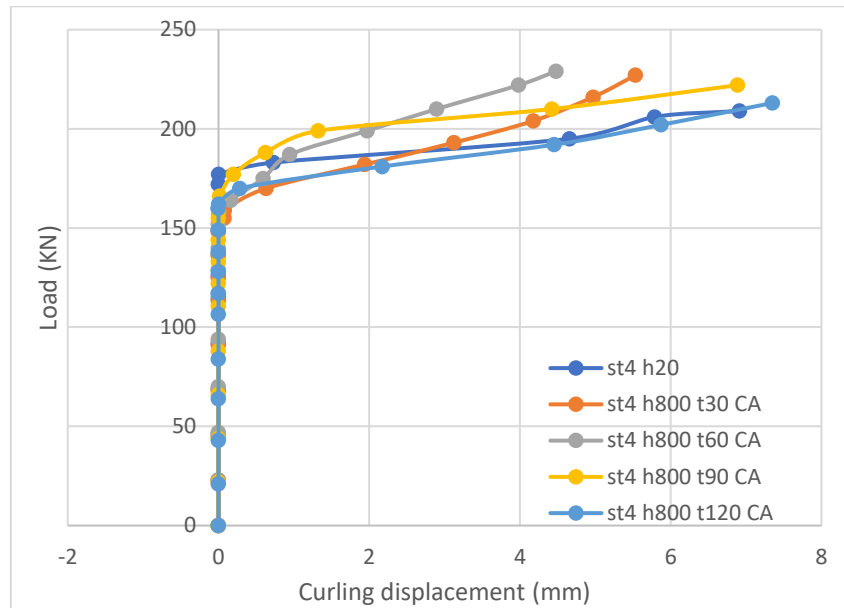
			load			
st4 h20	170	230	7	177	0.77	2.8
st4 h800 t30 CA	169	227	5.5	155	0.68	2.55
st4 h800 t60 CA	167	229	4.48	157	0.69	3.4
st4 h800 t90 CA	161	222	6.8	159	0.72	4.05
st4 h800 t120 CA	160	215	7.3	162	0.75	3.19



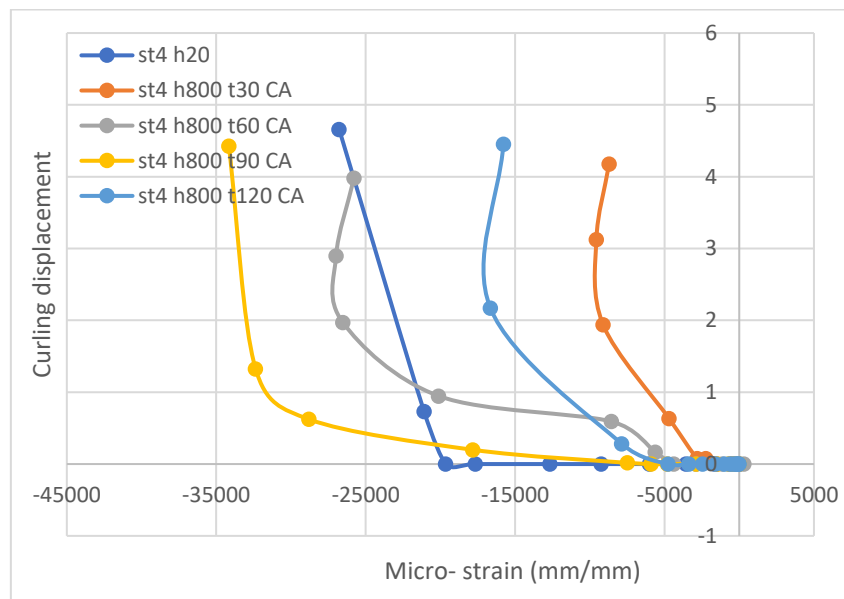
a- load vs Axial displacement



b- Load Vs Micro- strain



c- Load Vs Curling displacement



d- Curling displacement vs Micro-strain

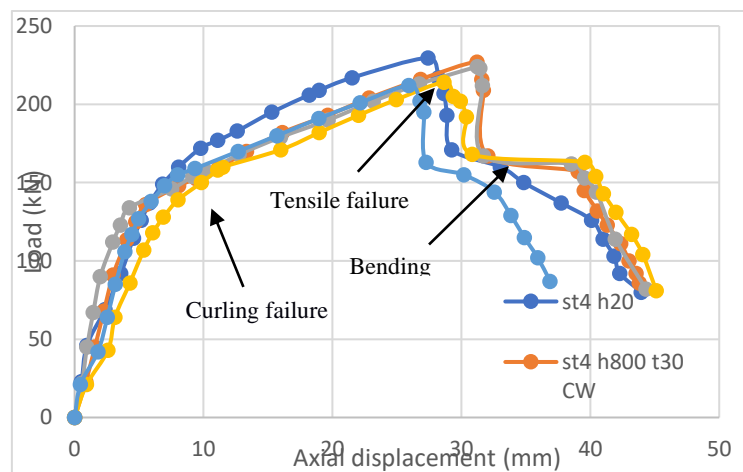
Figure (6) The results of heated and air-cooled 4 mm thick specimens at 800°C.

Table (2) presents the results of heating 4 mm thick, water-cooled specimens. The yield load increase with the increase in the heating period but remain it is lower than the load of the reference specimen. The ratio (P_{yt}/P_y) decreases with the increase in the heating period, where the highest ratio decrease is 12% in the heating time 30 minutes and the lowest decrease is 8% in the heating time 120 minutes. The ratio ultimate strength (P_{ut}/P_u) decreases with increase in the heating duration, it was 8% in 120min heating time. Figure (7-a) shows that the axial

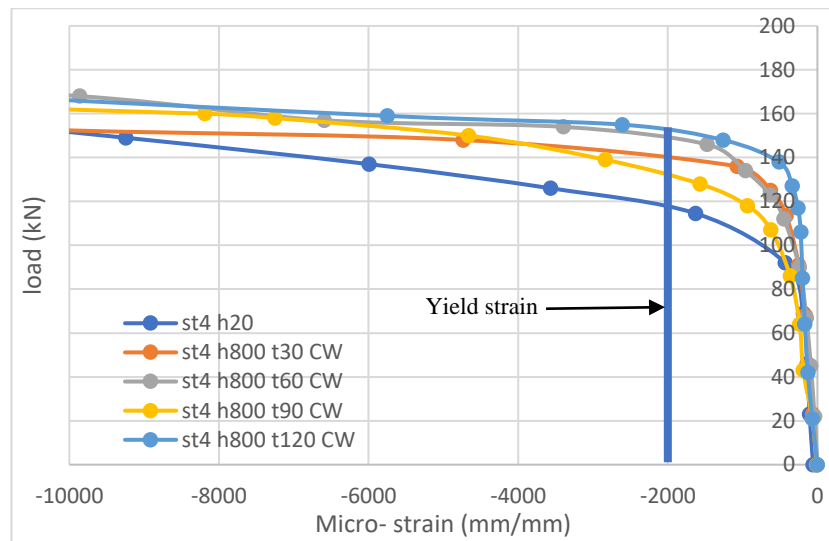
displacement was close to the displacement of the reference specimen until the time of heating 120 min, where it decreased significantly. The ductility increases with increasing the heating time to 60 min, then tend to drop with increasing heating duration to 120min. Figure (7-b) shows the relationship between strain and load where the yield strain of the heated specimens is close to the yield strain of the reference specimen. The curling load increase with the increase in the heating period. But the curling load remained less than the reference specimen. The ratio (P_c/P_u) increases with the increase in the heating period, where the highest ratio decrease is 10% in the heating time 30 minutes and the lowest decrease is 4% in the heating time 120 minutes. The curling displacement increased when the heating time was increased to 60 min compared to the reference sample and then tended to decrease when the heating time was increased to 120 min, as shown in Figure (7-c). After converting specimens to plastic zone, curling displacement appeared as shown in Figure (7-d).

Table (2) The results specimens thickness 4mm-800°C, water-cooled

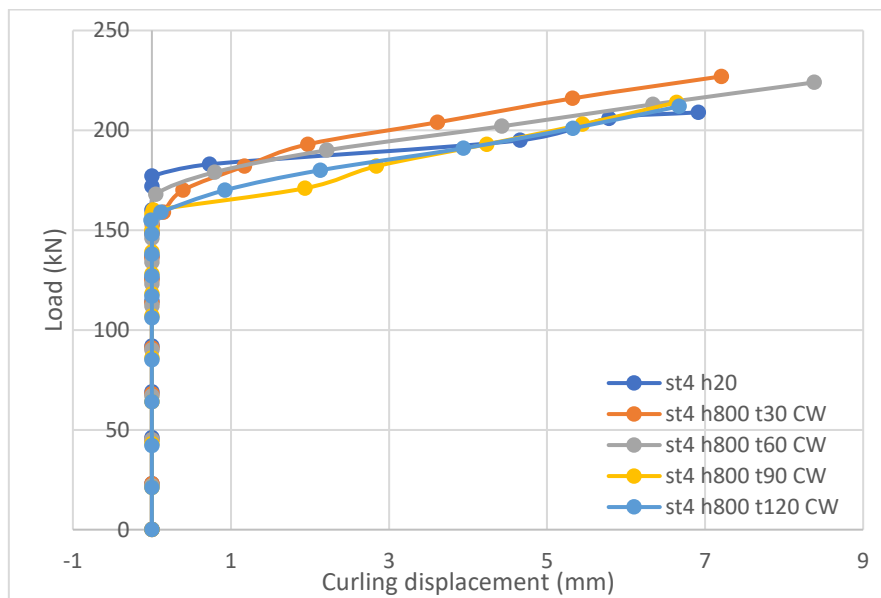
Specimen	Yielding Load P_y (kN)	Ultimate Load P_u (kN)	Curling displacement (mm) at max load	Curling Load P_c (kN)	P_c/P_u	Ductility
st4 h20	170	230	7	177	0.77	2.8
st4 h800 t30 CW	150	227	7.2	153	0.67	3.5
st4 h800 t60 CW	153	225	8.4	155	0.69	3.7
st4 h800 t90 CW	155	214	6.6	158	0.74	2.7
st4 h800 t120 CW	157	212	6.7	155	0.73	2.9



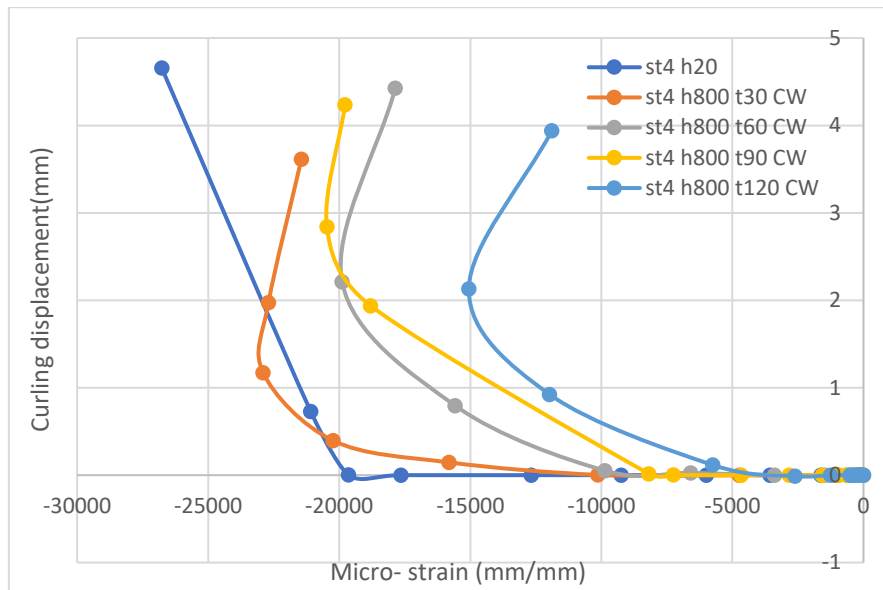
a- load vs Axial displacement



b- Load Vs Micro- strain



c- Load Vs Curling displacement



d- Curling displacement vs Micro- strain

Figure (7) The results of heated and water-cooled 4 mm thick specimens at 800°C.

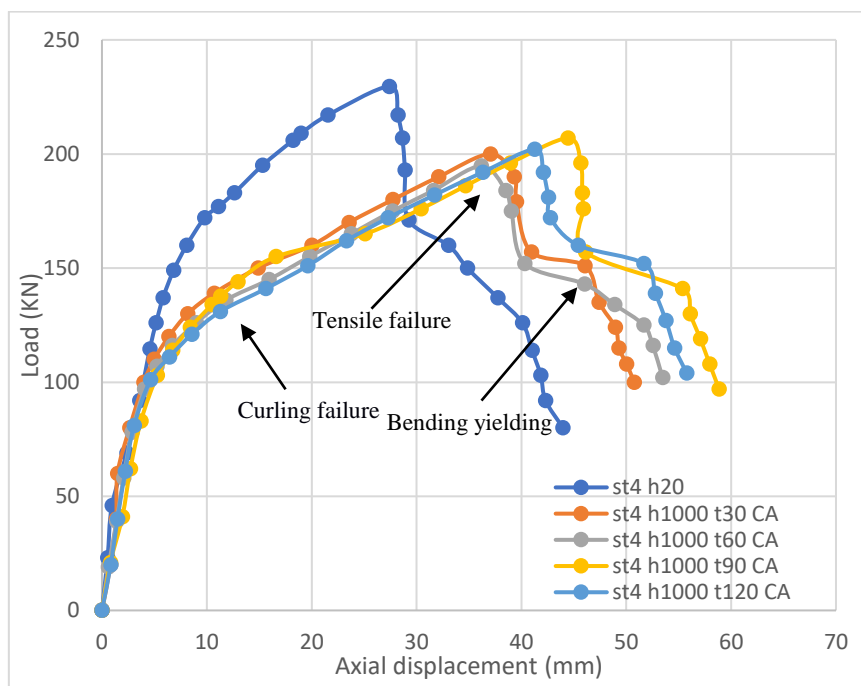
3.3 The Effect of Heating Time at 1000°C

Table (3) offers the results of specimens with a 4mm thickness heated to 1000°C and cooled in the air. The yield strength and ultimate strength decreased as the heating duration prolonged. After 120 minutes of heating, the yield strength ratio (P_{yt}/P_y) and the ultimate strength ratio (P_{ut}/P_u) dropped 28% and 12%, respectively. The axial displacement to specimens heated was higher than the displacement of the reference specimen, as shown in Figure (8-a), because the ductility increased as the heating duration increased. The yield strain of the heated specimens was lower than of the reference specimen, as shown in Figure (8-b), the strain dropped as the heating time increased. The curling load was lower than in the reference specimen. The ratio (P_c/P_u) dropped as the period of heating increased. After 120 minutes of heating, the ratio declined by 12%. Figure (8-c) illustrates that curling displacement stays close to the reference specimen as the heating duration increases. When converting specimens to plastic zone, curling displacement appeared in Figure(8-d).

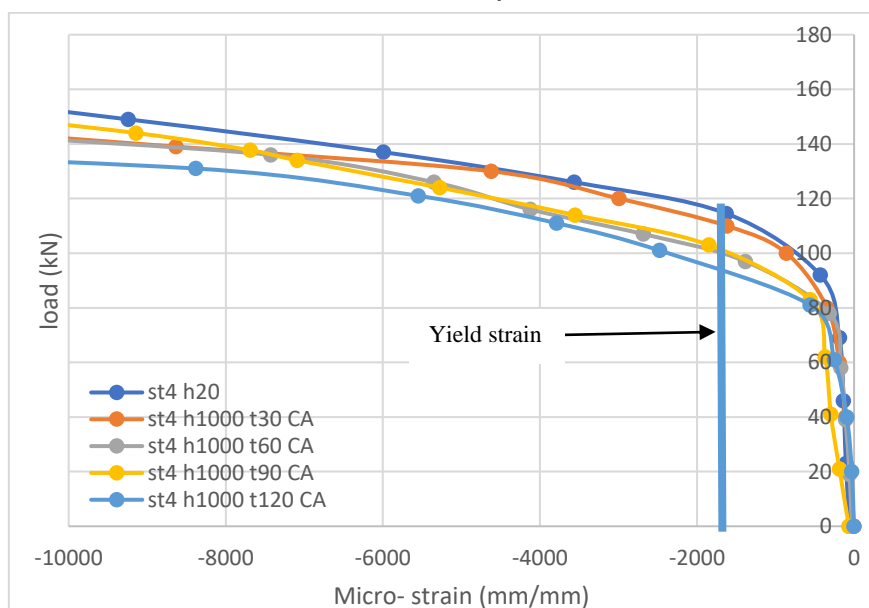
Table (3) The results specimens thickness 4mm-1000°C, air-cooled

Specimen	Yielding Load P_y (kN)	Ultimate Load P_u (kN)	Curling displacement (mm) at max load	Curling Load P_c (kN)	P_c/P_u	Ductility

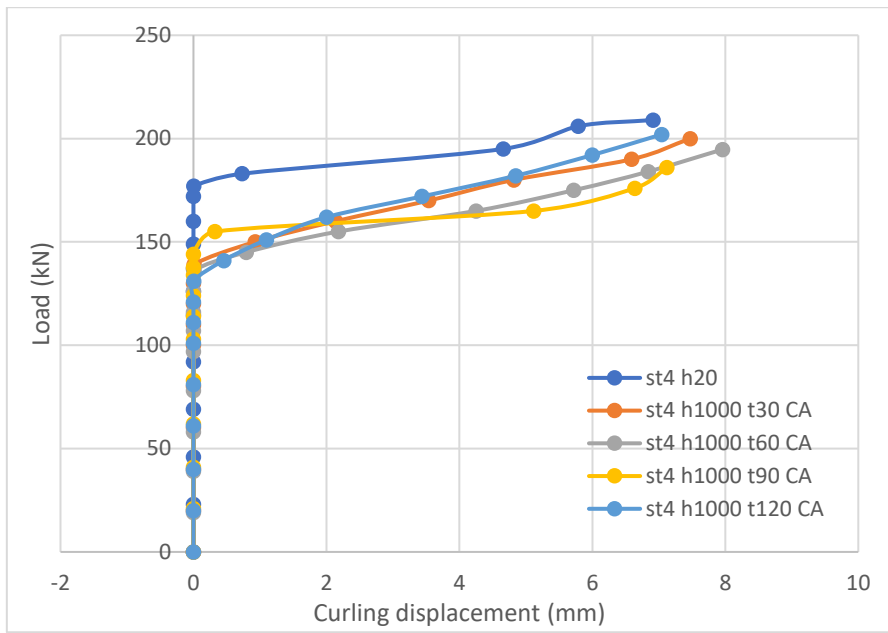
st4 h20	170	230	7	177	0.77	2.8
st4 h1000 t30 CA	135	200	7.47	139	0.7	3.85
st4 h1000 t60 CA	131	195	7.95	136	0.7	3.42
st4 h1000 t90 CA	128	207	7.12	137	0.66	5.15
st4 h1000 t120 CA	123	202	7.04	132	0.65	4.64



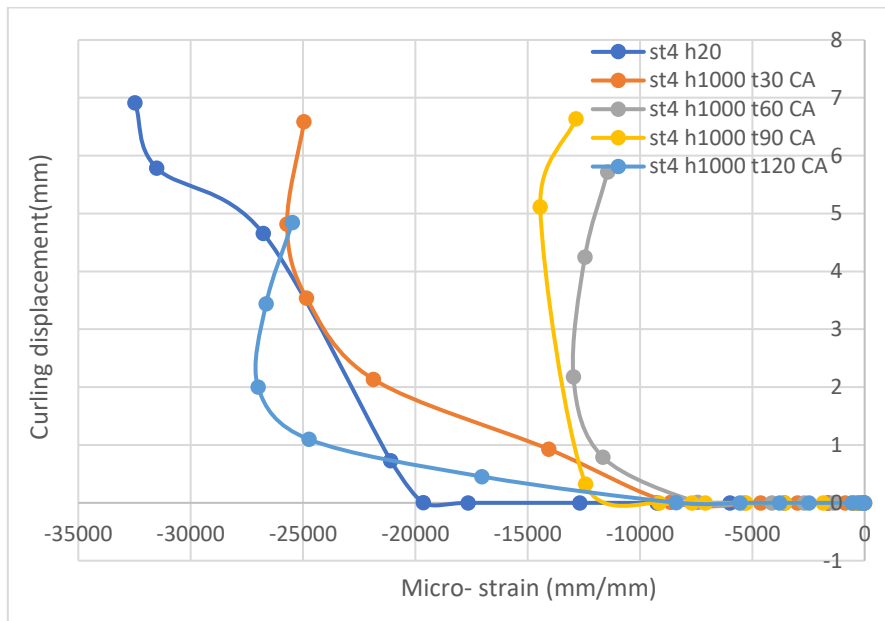
a- load vs Axial displacement



b- Load Vs Micro- strain



c- Load Vs Curling displacement



d- Curling displacement vs Micro- strain

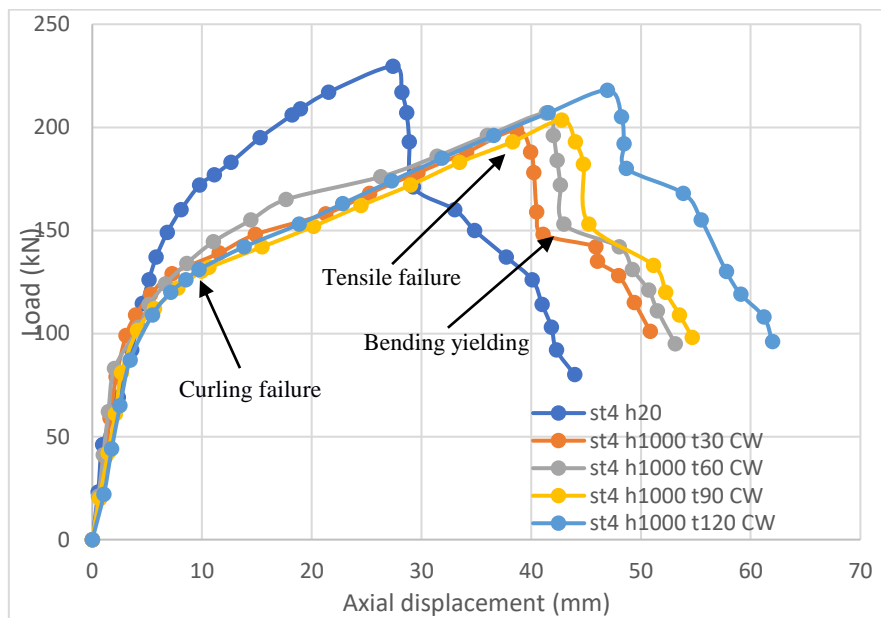
Figure (8) The results of heated and air-cooled 4 mm thick specimens at 1000°C.

Table (4) presented the results of 4mm thickness specimens heated to 1000°C and cooled in water. The yield load decrease with the increase in the heating period. The ratio (P_{yt}/P_y) decreases with the increase in the heating period, of 28% in the heating time 120 min. The ultimate strength ratio (P_{ut}/P_u) decreases in heating time in 30 min by 13%, but the decrease improves to 5% with an increased heating duration to 120 min. Figure (9-a) shows that the axial displacement increase with increased heating duration. The ductility increases with increasing

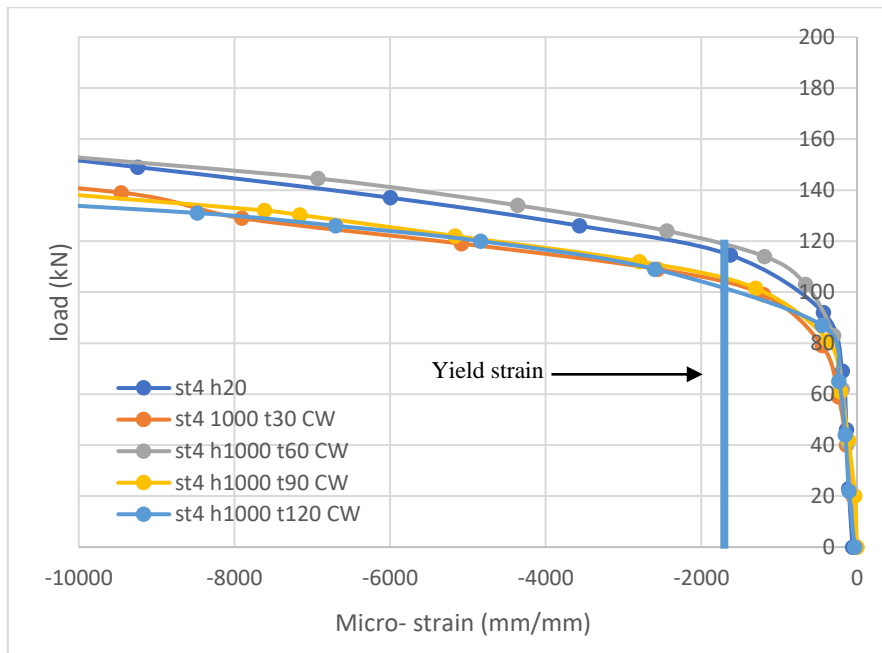
the heating time. Figure (9-b) illustrates the relationship between strain and load for heated specimens was lower than that of the reference specimen. The curling load decrease with the increase in the heating duration. The ratio (P_c/P_u) decreases with the increase in the heating period, is 16% in the heating time 120 min. The displacement of the curling remained close to the displacement of the reference specimen despite the increase in the heating period, as shown in Figure (9-c). Curling displacement occurred after yielding specimens, as shown in Figure (9-d).

Table (4) The results specimens thickness 4mm-1000°C, water-cooled

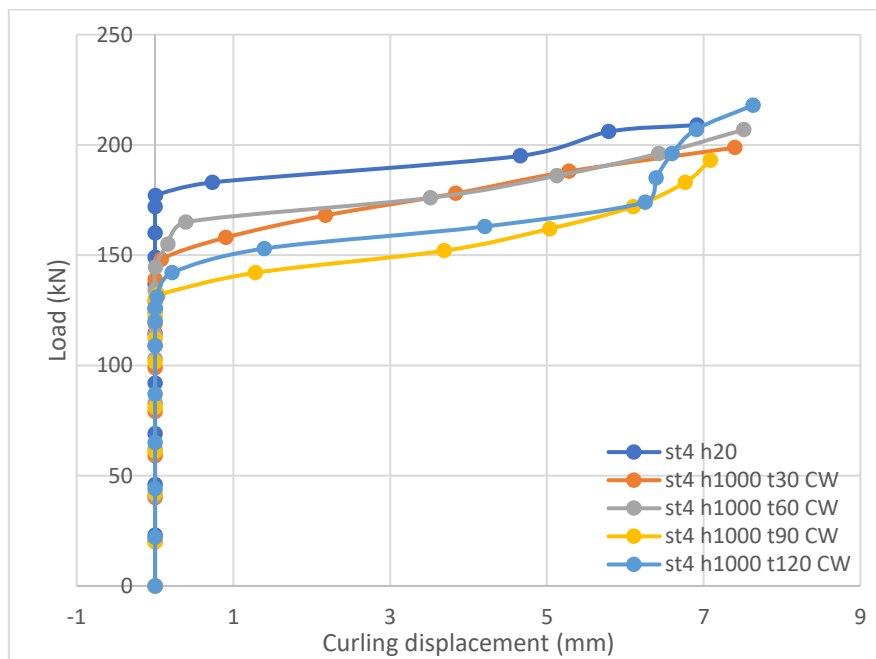
Specimen	Yielding Load P_y (kN)	Ultimate Load P_u (kN)	Curling displacement (mm) at max load	Curling Load P_c (kN)	P_c/P_u	Ductility
st4 h20	170	230	7	177	0.77	2.8
st4 h1000 t30 CW	136	199	7.39	148	0.74	3.47
st4 h1000 t60 CW	135	207	7.51	145	0.70	4.68
st4 h1000 t90 CW	124	204	7.08	131	0.65	5.16
st4 h1000 t120 CW	122	218	7.63	126	0.61	6.21



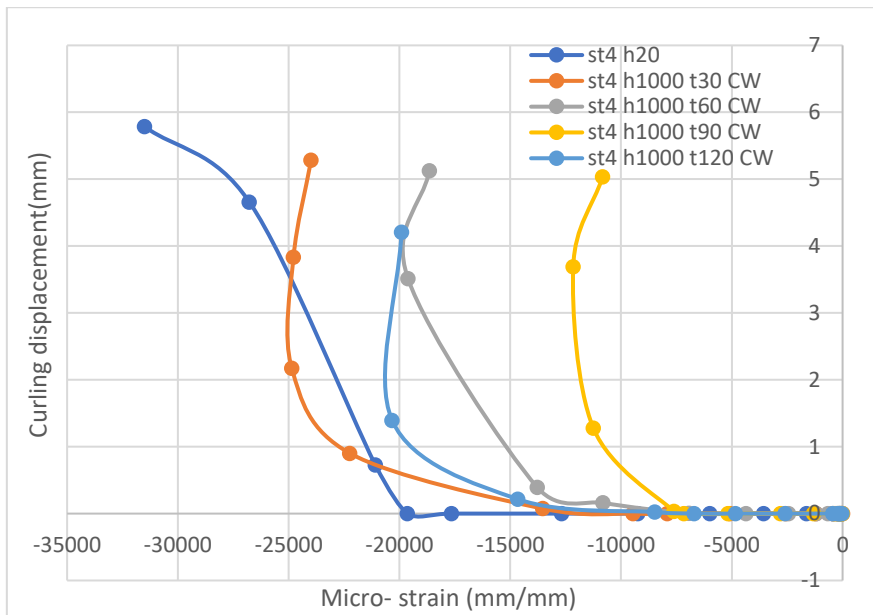
a- load vs Axial displacement



b- Load Vs Micro- strain



c- Load Vs Curling displacement



d- Curling displacement vs Micro- strain

Figure (9) The results of heated and water-cooled 4 mm thick specimens at 1000°C.

3.4 Mathematical Analysis of Specimens

The failure mode was the same for all specimens examined. The specimens failed by curling failure, net tensile fracture, net shear yielding, and bending yielding, as shown in Figure (10).

Curling Bending yielding Net shear yielding Net tensile fracture

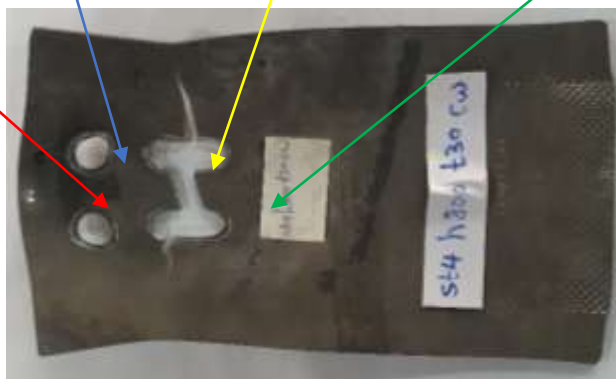


Figure (10) Failure mode

The American Institute of Steel Construction (2017) "Henrietta (2017)" approach for carbon steel were used to compute the ultimate strength of the tested specimens. However, the bending yielding was added to the model.

$$P_{usc} = P_{ut} + P_{ys} + P_{yb}$$

P_{usc} = the ultimate strength of the connection.

P_{ut} = the net tensile fracture strength = $A_{nt} \times F_u$

P_{ys} = the net shear yielding strength = $A_{ns} \times 0.6F_y$

P_{yb} = the net bending yielding strength = $A_{nb} \times F_y$

A_{nt} = the net tensile fracture area = $(g - d) \times t$

A_{ns} = the net shear yielding area = $(p - d) \times t$

A_{nb} = the net bending yielding area = $(e - d) \times t$

F_y = the yield stress of coupon steel.

F_u = the ultimate stress of coupon steel.

g = the distance between the centre of the bolts perpendicular to the tension axis.

P = the distance between the centre of the bolts parallel to the axis of tension.

e = the distance between the centre of the bolts parallel to the axis of tension and the edge of the specimen.

t = thickness of the specimen.

d = the hole diameter.

The results presented in Table (5) show that the ASIC approach underestimates the connection strength.

Table (5): Experimental results versus AISC

NO	Specimens	Thickness (mm)	F_y N/mm ²	F_u N/mm ²	P_{uexp} kN	P_{usc} kN	Ratio P_{usc}/P_{uexp}
1	Cst4 h20	4	312	780	230	168.1	0.73
2	Cst4 h800 t30 CA	3.87	254	785	227	144.6	0.64
3	Cst4 h800 t30 CW	3.87	253	806	227	145.98	0.64
4	Cst4 h800 t60 CA	3.88	248	773	229	142.1	0.62
5	Cst4 h800 t60 CW	3.87	264	814	225	150.13	0.67
6	Cst4 h800 t90 CA	3.88	258	791	222	146.73	0.66
7	Cst4 h800 t90 CW	3.87	248	790	214	143.1	0.67
8	Cst4 h800 t120 CA	3.88	255	771	215	144.15	0.67
9	Cst4 h800 t120 CW	3.86	235	754	212	135.7	0.64
10	Cst4 h1000 t30 CA	3.88	304	761	200	158.96	0.79
11	Cst4 h1000 t30 CW	3.88	257	793	199	146.58	0.74
12	Cst4 h1000 t60 CA	3.85	298	773	195	156.81	0.80
13	Cst4 h1000 t60 CW	3.86	274	797	207	151.54	0.73
14	Cst4 h1000 t90 CA	3.83	289	780	207	153.72	0.74
15	Cst4 h1000 t90 CW	3.85	225	780	204	134.27	0.66

16	Cst4 h1000t120CA	3.8	307	766	202	157.02	0.78
17	Cst4h1000t120 CW	3.81	221	726	218	127.3	0.58

4. Conclusion

Experimental research was carried out on the behaviour of stainless steel bolted connections after exposure to high-temperature heating at different periods of time, as it heated to 800°C and 1000°C. The heating affects the stainless steel thickness but does not affect other dimensions. This thickness difference affects the stainless steel cross-section and load-bearing ability. At heating to 1000°C, crusts obviously appeared on the surface of the coupons and specimens. no appeared surface corrosion for any heating temperature or duration to both cooling methods. The curling displacement decrease as the heating temperature increases. The ultimate strength decreased by 7% and 12%, respectively, when the specimens were heated to a temperature of 800°C and 1000°C and cooled by air. It decreases by 8% and 5% when heated to a temperature of 800°C and 1000°C and cooled with water. There was no significant effect of the cooling method on ultimate load. Heating stainless steel to a temperature of 800°C did not affect its durability until the time of heating 90 minutes, but the effect began to increase when heating for 120 minutes. The effect was evident when heating to a temperature of 1000°C. The endurance of water-cooled specimens did not have a significant difference from that of air-cooled specimens, so stainless steel is more resistant to temperature and for a longer time. The AISC approach underestimates the connection post-fire strength.

Reference

1. Ahmed, A., & Teh, L. H. J. J. o. C. S. R. (2019). Thread effects on the stiffness of bolted shear connections. *160*, 77-88.
2. Baddoo, N. J. J. o. c. s. r. (2008). Stainless steel in construction: A review of research, applications, challenges and opportunities. *64*(11), 1199-1206.
3. Beitel, J. J., & Iwankiw, N. (2008). *Analysis of needs and existing capabilities for full-scale fire resistance testing*. US Department of Commerce, Technology Administration, National Institute of
4. Bouchaïr, A., Averseng, J., & Abidelah, A. (2008). Analysis of the behaviour of stainless steel bolted connections. *Journal of Constructional Steel Research*, *64*(11), 1264-1274. doi:<https://doi.org/10.1016/j.jcsr.2008.07.009>

5. Cai, Y., & Young, B. (2018). Fire resistance of stainless steel single shear bolted connections. *Thin-Walled Structures*, *130*, 332-346.
doi:<https://doi.org/10.1016/j.tws.2018.05.004>
6. Cai, Y., & Young, B. (2020). Effects of end distance on thin sheet steel single shear bolted connections at elevated temperatures. *Thin-Walled Structures*, *148*, 106577.
doi:<https://doi.org/10.1016/j.tws.2019.106577>
7. EN, B. J. B. S. I. (2001). 10002-1, "Metallic materials tensile testing, Part 1: method of test at ambient temperature" .
8. He, K., Chen, Y., & Han, S. J. J. o. C. S. R. (2019). Experimental investigation of square stainless steel tubular stub columns after elevated temperatures. *159*, 397-414.
9. He, Y. C., & Wang, Y. C. J. T.-W. S. (2016). Load-deflection behaviour of thin-walled bolted plates in shear at elevated temperatures. *98*, 127-142.
10. Henrietta, B. (2017). *Specification for Structural Steel Buildings*. Retrieved from United States of America: <https://policycommons.net/artifacts/1738130/specification-for-structural-steel-buildings/>
11. Kim, G., Kim, T., Hwang, B., & Kim, J. J. T.-W. S. (2020). Ultimate strength of lean duplex stainless steel single-shear bolted connections with four bolts. *155*, 106950.
12. Kim, T., Jeong, H., & Cho, T. (2011). The finite element analysis of the ultimate behavior of thin-walled carbon steel bolted connections. *Journal of Constructional Steel Research*, *67*(7), 1086-1095. doi:<https://doi.org/10.1016/j.jcsr.2011.01.004>
13. Kim, T., Yoo, J., & Roeder, C. W. (2015). Experimental investigation on strength and curling influence of bolted connections in thin-walled carbon steel. *Thin-Walled Structures*, *91*, 1-12. doi:<https://doi.org/10.1016/j.tws.2015.01.016>
14. Kim, T. S., & Kuwamura, H. J. T.-W. S. (2007). Finite element modeling of bolted connections in thin-walled stainless steel plates under static shear. *45*(4), 407-421.
15. Liu, H., Liu, D., Chen, Z., & Yu, Y. (2017). Post-fire residual slip resistance and shear capacity of high-strength bolted connection. *Journal of Constructional Steel Research*, *138*, 65-71. doi:<https://doi.org/10.1016/j.jcsr.2017.06.026>
16. Mahmood, M., Elamin, A., & Tizani, W. (2020). Ultimate strength and fracture sequence of bolted connections to thin-walled carbon steel. *Structures*, *23*, 646-659.
doi:<https://doi.org/10.1016/j.istruc.2019.11.011>
17. Rossi, B. J. T.-W. S. (2014). Discussion on the use of stainless steel in constructions in view of sustainability. *83*, 182-189.

18. Sobrinho, K. d. P., da Silva, A. T., Rodrigues, M. C., Henriques, J. A., Vellasco, P. C. G. d. S., & de Lima, L. R. O. (2022). A comprehensive assessment of curling effects in stainless steel bolted connections. *Thin-Walled Structures*, 176, 109387.
doi:<https://doi.org/10.1016/j.tws.2022.109387>
19. Yang, K.-C., Hsu, R.-J., & Hsu, C.-F. J. I. J. o. S. S. (2013). Effect of end distance and bolt number on bearing strength of bolted connections at elevated temperature. *13*(4), 635-644.